Study of Bulk and Elementary Screw Dislocation Assisted Reverse Breakdown in Low-Voltage (< 250 V) 4H-SiC p^+n Junction Diodes - Part 1: DC Properties

Philip G. Neudeck (Member, IEEE)

NASA Lewis Research Center, M.S. 77-1, 21000 Brookpark Road, Cleveland, OH 44135

Wei Huang and Michael Dudley

Department of Materials Science and Engineering, State University of New York at Stony Brook, Stony Brook, NY 11794-2275

Abstract

Given the high density (~ 10^4 cm^{-2}) of elementary screw dislocations (Burgers vector = 1c with no hollow core) in commercial SiC wafers and epilayers, all appreciable current (> 1 A) SiC power devices will likely contain elementary screw dislocations for the foreseeable future. It is therefore important to ascertain the electrical impact of these defects, particularly in high-field vertical power device topologies where SiC is expected to enable large performance improvements in solid-state high-power systems. This paper compares the DC-measured reverse-breakdown characteristics of low-voltage (< 250 V) small-area (< 5 x 10^{-4} cm^2) 4H-SiC p^+n diodes with and without elementary screw dislocations. Compared to screw dislocation-free devices, diodes containing elementary screw dislocations exhibited higher pre-breakdown reverse leakage currents, softer reverse breakdown I-V knees, and highly localized microplasmic breakdown current filaments. The observed localized 4H-SiC breakdown parallels microplasmic breakdowns observed in silicon and other semiconductors, in which space-charge effects limit current conduction through the local microplasma as reverse bias is increased.

INTRODUCTION

The inherent physical properties of silicon carbide (SiC) are extremely well-suited for power semiconductor electronic devices. These include a higher breakdown field (> 5 times that of Si) that permits much smaller drift regions (i.e., much lower drift region resistances), a higher thermal conductivity (> 3 times that of Si) that permits better heat dissipation, and a wide bandgap energy (2.9 eV for 6H-SiC, 3.2 eV for 4H-SiC) that enables higher junction operating temperatures [1]. Theoretical appraisals have suggested that SiC power MOSFET's and diode rectifiers would operate over higher voltage and temperature ranges, have superior switching characteristics, and yet have die sizes nearly 20 times smaller than correspondingly rated silicon-based devices [2]. This would enable large power system performance improvements, which has fueled speculation that SiC may someday supplant silicon in many high-power electronic applications [3]. Before this can occur however, SiC power semiconductor components must demonstrate capabilities that are commonplace to well-developed silicon power components in use today. As a simplistic minimum, high-power solid-state devices must: 1) block high voltages in the off-state with negligible leakage current, 2) carry high on-state currents with minimal parasitic voltage drop, 3) rapidly switch back-and-forth between on-state and off-state, 4) function reliably without a single failure over the operational lifetime of the system, and 5) be cost-effective to mass produce and incorporate into high power systems. While some prototype SiC power devices produced to date meet one or two of these 5 criteria, SiC devices that meet even a majority of these criteria do not as yet exist.

It is widely recognized that material quality deficiencies are the primary reason why SiC high-power devices cannot be realized at present. Almost all SiC power electronics are being developed on commercially available c-axis 6H- and 4H-SiC wafers whose surfaces lie roughly perpendicular (to within 10°) of the crystallographic c-axis. Efforts to make mass-producible wafers and devices oriented in other SiC polytypes and other crystallographic directions have to date proven much less-acceptable for high-field device performance than c-axis oriented 4H- and 6H-SiC wafers and epilayers [4]. While small-current, small-area high-voltage (1-5 kV) SiC devices are being prototyped and tested, the high densities of crystallographic defects in SiC wafers prohibits the

attainment of SiC devices with very high operating currents (> 50 A) that are commonly obtainable in silicon-based high-power electronics [1, 5]. Micropipe defects are clearly very detrimental to electrical device performance, as these defects cause premature breakdown point-failures in SiC high-field devices fabricated in 4H- and 6H-SiC c-axis crystals with and without epilayers [5]. Commercial 4H- and 6H-SiC wafers and epilayers also contain elementary screw dislocations (i.e., Burgers vector = 1c with no hollow core) in densities on the order of thousands per cm^2, nearly 100-fold micropipe densities [6-9]. Because of the non-terminating behavior of screw dislocations, both hollow-core (micropipes) and non-hollow-core (elementary) screw dislocations and associated crystal lattice stresses are replicated in subsequently grown SiC epilayers [10, 11].

The electrical impact of elementary screw dislocation defects on SiC device performance has largely been overlooked while attention has largely focused on eradicating SiC micropipes. However as SiC micropipe densities fall below 1 per cm^2 in the best reported wafers [12], the operational effects of elementary screw dislocations must now be considered. While not nearly as detrimental to SiC device performance as micropipes, it has recently been demonstrated that elementary screw dislocations somewhat degrade the reverse leakage and breakdown properties of low-voltage (< 250 V) 4H-SiC p^+n diodes [13]. Diodes containing elementary screw dislocations exhibited higher pre-breakdown reverse leakage current, softer reverse breakdown I-V knee, and highly localized microplasmic breakdown current filaments.

Localized breakdowns and high-current filaments at junction hotspots are undesirable in silicon-based solid-state power devices. In operational practice, silicon power devices that uniformly distribute breakdown current over the entire junction area exhibit much greater reliability than silicon devices that manifest localized breakdown behavior. This is because silicon devices that avoid localized junction breakdown exhibit larger Safe Operating Areas (SOA's) and can much better withstand repeated fast-switching stresses and transient overvoltage glitches that arise in high-power systems [14-17]. Positive temperature coefficient of breakdown voltage (PTCBV), a standard behavior in silicon power devices free of crystal dislocation defects, helps insure that current flow is distributed uniformly throughout a device, instead of concentrated at high-current

filaments. This enables silicon power rectifiers to exhibit a high energy to thermal junction failure when subjected to transient breakdown or switching bias conditions in which voltage and current are simultaneously large in the device. It is generally accepted that power rectifier SOA and reliability increases with increasing semiconductor junction energy to fail. Silicon junctions that suffer localized breakdown due to the presence of crystal dislocation defects do not generally exhibit sufficient energy to fail characteristics to be considered reliable for use in high-power systems.

Before SiC can become feasible for widespread incorporation into high-power systems, SiC power devices must demonstrate at least equal, if not superior, reliability characteristics as present-day dislocation defect-free silicon power devices. Therefore, SiC power devices must demonstrate at least equal (probably superior) SOA's and immunity to switching and overvoltage stresses as silicon power devices. Since all appreciable current (> 1 A) SiC power devices manufactured on commercial SiC wafers are virtually guaranteed to contain elementary screw dislocations for the foreseeable future, it is important to ascertain the junction breakdown and energy-to-fail properties of SiC diodes with elementary screw dislocations.

This paper examines the DC-measured reverse breakdown characteristics of low-voltage 4H-SiC p^+n junction diodes with and without elementary screw dislocations. Experimental data reviewing and enhancing the Ref. [13] observations of microplasmic breakdown current filaments at elementary screw dislocations is presented. The observed behavior parallels microplasmic breakdowns previously observed in silicon and other semiconductor pn junction diodes.

EXPERIMENT

Epitaxial mesa-isolated 4H-SiC p^+n junction diodes cross-sectionally depicted in Fig. 1 were fabricated on commercial substrates as previously described in Ref. [13]. Circular and rectangular diode mesas ranging in area from 7×10^{-6} cm^2 to 4×10^{-4} cm^2 were defined by RIE to a depth of 2 - 3 μm. Synchrotron White Beam X-ray Topography (SWBXT) was employed on to map the exact

locations of elementary screw dislocations within each mesa diode [6, 7, 18]. Figure 2 displays enlarged SWBXT back-reflection images of two typical rectangular devices. The light spots residing inside the Figure 2b mesa indicate the presence of an elementary screw dislocations of Burgers vector 1c with no hollow core [9], whereas there is no such defect present in the Figure 2a rectangular mesa diode.

The sample was initially measured with no contact metallizations in low-light conditions that permitted the clear observation and pinpointing of breakdown bias luminescence with respect to device boundaries. Sufficient electrical connection to the diodes for these low-current (< 10 mA) measurements was obtained by directly probing the degenerately-doped p^+ epilayer topside and contacting wafer backside with the probe station chuck. All DC measurements were conducted in air on diodes with breakdown voltages below 150 V, in which there was no interference from edge-related breakdown phenomena such as surface flashover.

Figure 3 shows the DC reverse-bias I-V characteristics of devices with and without screw dislocations on a logarithmic current scale. To minimize the effects of nonuniform doping present across the wafer, the devices measured in this figure all reside within 1 mm of each other on the wafer. Below 60 V applied reverse bias, the leakage current of diodes with and without screw dislocations were below the current noise floor of the measurement apparatus. At around 65 V reverse bias, diodes containing at leas one elementary screw dislocation exhibit a very sharp rise in current in Figure 3, while the reverse leakage of the screw dislocation-free diodes remains below the measurement noise floor until around 90 V applied bias. Coinciding with the sharp, several order of magnitude current rise for diodes with screw dislocations (at around 65 V for diodes plotted in Figure 3), one or more concentrated breakdown microplasmas becomes optically observable. Microplasmas are clearly visible in the Figure 4 low-light optical micrograph of the Figure 2b diode under 85 V applied reverse bias. Direct comparison of Figures 2b and 4 shows that the locations of the breakdown microplasmas in Figure 4 coincides with the locations of elementary screw dislocation revealed by SWBXT in Figure 2b. No microplasmas were observed in screw dislocation-free diodes, even when the devices were biased well into breakdown at more

than 95 V applied reverse bias. Instead, the screw-dislocation free devices exhibited reasonably uniform breakdown luminescence distributed over the entire mesa when a few mA of breakdown current is drawn. When biased beyond 95 V, diodes with screw dislocations also exhibit bulk breakdown luminescence distributed over the mesa area in addition to the bright localized microplasma.

Detailed comparisons of the I-V, SWBXT, and breakdown luminescence characteristics of dozens of devices on the same 4H-SiC wafer have been carried out to date. Without exception, all devices that SWBXT identified as containing at least one elementary screw dislocation (without screw dislocations larger than 1c Burgers vector) exhibited degraded reverse I-V characteristics and breakdown-bias microplasmas located at 1c screw dislocations. It can be noted from Figure 3 that there was some noticeable scatter in microplasma turn-on voltages, sometimes observed between different screw dislocations residing within a single device. These observations are consistent with the electrical and optical measurements in Ref. [19], except that Konstantinov et. al. did not attribute breakdown microplasmas to elementary screw dislocations, for reasons discussed in [13].

Figure 5 shows the temperature dependent reverse I-V knee characteristics of two 50 μm diameter diodes located next to each other on the wafer, one free of elementary screw dislocations and the other containing two elementary screw dislocations. Prior to microplasma turn-on the dislocation-free diode clearly exhibits superior smaller reverse leakage current. Over the measured temperature range of 298 K to 673 K, the DC breakdown characteristics of both diodes exhibit only small changes which are barely discernible in Figure 5. For low current levels between 0.5 μA and 50 μA where device self-heating is minimized, both diodes exhibit a small drop in apparent breakdown voltage from 298 K to 473 K, followed by a small increase in breakdown voltage when the temperature is further increased from 473 K to 673 K. Reversal of SiC breakdown temperature coefficient from negative to positive at higher temperatures is consistent with previous work [20-22], but it is particularly noteworthy for the diode with screw dislocations in which all breakdown current is flowing through microplasmas over this current range.

Once bias is increased beyond the bulk breakdown voltage, bulk avalanche current increases at a much faster rate than the microplasma current (as observed in Figure 5), so that bulk breakdown quickly dominates total breakdown current measured at larger reverse biases. When tested with a 60 Hz curve-tracer, devices with and without screw dislocations were both briefly able to withstand peak breakdown current densities (normalized to entire device area) as high as 1000 A/cm^2, corresponding to peak power densities as high as 140 kW/cm^2.

DISCUSSION

Based partly on localized breakdown phenomena previously observed in other semiconductors [23, 24], there are several possible mechanisms for localized breakdown which might be applicable to the 4H-SiC elementary screw dislocation breakdown observed in this work. Lattice deformation around an elementary screw dislocation is likely to somewhat change the semiconductor band structure in the vicinity of the defect. If this leads to a local reduction in the effective 4H-SiC bandgap near an elementary screw dislocation, carriers would require slightly less energy to impact ionize, and the probability of breakdown due to carrier tunneling would also increase [14]. Without changing the bandgap itself, other local band structure changes may influence high-field carrier transport and scattering so as to effectively reduce the semiconductor critical field in the near-defect region. The presence of dangling bonds down the core of the screw dislocation may also play a key role in the defect-assisted breakdown process. Another speculation is that enhanced impurity incorporation may arise as the 1c screw dislocation propagates during epilayer growth, which would result in higher doping or deep level impurities near the dislocation that would locally reduce breakdown voltage. It is worth noting that work by Si et. al. [8, 9] has previously shown that many elementary screw dislocations do not run exactly parallel to the crystallographic c-axis, but instead can lie at angles up to 15° from parallel to the c-axis. Differing angles between the elementary screw dislocations and the applied electric field may therefore account for observed differences in microplasma turn-on voltages. The small increase in microplasma turn-on voltage between 473 K and 673 K in Figure 5 is particularly notable, because it suggests that the localized

breakdown may exhibit locally stable PTCBV behavior at high temperatures, albeit at a lower voltage than the bulk defect-free areas of the junction. A more complete understanding of the elementary screw dislocation breakdown physics will require further studies.

Between the microplasma turn-on voltage and the bulk breakdown voltage (~65 V < V < ~90 V in Figure 3, ~51 V < V < ~71 V in Figure 5), essentially all measured current is flowing through individual microplasmas. The measured I-V behavior of these microplasmas is strikingly similar to localized defect-assisted breakdown previously observed in silicon and other semiconductors. Detailed reviews of localized semiconductor breakdown physics are given by Barnett and Chynoweth [23-26]. As discussed by Barnett [26], the current-voltage characteristic of a localized breakdown current filament is typically normalized by subtracting the junction voltage. At sufficient reverse bias beyond the microplasma turn-on, conduction at high current density through a localized breakdown current filament becomes space-charge limited. The microplasma current follows the well-known power-law behavior for space-charge limited conduction with respect to the normalized voltage V_N:

$$I \alpha V_N^{1.5\text{-}2.0} \qquad (1)$$

Because all measured current between turn-on of all microplasmas and the onset of bulk breakdown is flowing through microplasmas at screw dislocations, it is appropriate to normalize current with respect to number of microplasmas instead of normalizing to junction area. Figure 6 shows a plot of normalized current I_N (i.e., current per microplasma) vs. normalized voltage V_N (i.e., voltage beyond first microplasma turn-on) for 9 4H-SiC devices with one or more screw dislocations. The voltage V_N for each 4H-SiC device was normalized by subtracting the voltage at which 1 μA of current was drawn by the first microplasma, consistent with where a sharp current increase is first registered in each diode. For reference, an empirical $I \alpha V^2$ fit to the measured data:

$$I_N = 0.8 (V_N - 3)^2 \mu A \qquad (2)$$

is also plotted in Figure 6. All microplasma I-V's exhibited $I \alpha V^2$ space-charge limited behavior prior to the onset of bulk breakdown. Relation (2) models almost all microplasmas measured in this work to within a factor of 2, even between diodes where un-normalized microplasma turn-on

voltages differed by as much as 20 V. The empirical $I \alpha V^2$ fit given in Figure 5 is consistent with Relation (2) for a diode containing two screw dislocations.

Prior to the onset of space charge limited conduction (SCLC), the steepness of current increase associated with initial microplasma turn-on (at around 65 V in Figure 3) is comparable to the steepness of current increase associated with bulk breakdown (at around 95 V in Figure 3) in microplasma-free diodes. In larger-area diodes containing numerous elementary screw dislocations, tens of milliamps of current could be drawn through microplasmas in parallel prior to the onset of microplasma SCLC and bulk junction breakdown. It is therefore possible to mistake the onset of localized microplasma breakdown for the onset of bulk avalanche breakdown, especially since almost all devices are characterized with contact metallizations that obscure the optical observation of localized breakdown microplasmas. Given that most published reports of 4H-SiC pn junction breakdown I-V's do not show more than a few milliamps of total breakdown current, the possibility that many workers are observing localized breakdown at elementary screw dislocations instead of the onset of bulk avalanche breakdown cannot immediately be ruled out. Similarly, if the reverse I-V characteristic is recorded on too large of a linear current scale (e.g., Figure 5 data plotted on a 10 mA/division linear current scale), it would become difficult to observe the softening of the breakdown knee for a device containing only one elementary screw dislocation.

The visible microplasmas observed in these measurements were no more than 3 μm in radius at maximum bias prior to bulk breakdown. While the I-V behavior of the 4H-SiC microplasmas is similar to previously observed microplasmas in other semiconductors, it should be noted that the 4H-SiC microplasma radii are considerably smaller than microplasma radii reported in silicon and GaAs [26]. Simplistically assuming uniform current flow over the 3 μm radius, one can estimate an effective breakdown area of 2.83×10^{-7} cm^2 for each elementary screw dislocation. In Figure 3 for example, almost all of the breakdown current between ~ 65 V and ~ 90 V appears to be flowing through less than 1% of the total pn junction area. At 0.5 mA of reverse breakdown current at 85 V

reverse bias (Figure 3), this corresponds to a first-order localized power density estimate of around 150 kW/cm^2 at the screw dislocation defect.

As discussed in the introduction, localized breakdowns and high current density filaments like those observed in this work are generally undesirable in solid-state power devices. Nevertheless, the localized breakdown did not appear to damage any of the 4H-SiC junctions tested in this work. In this low-voltage 4H-SiC p^+n diode sample, the localized breakdown power density at screw dislocations was apparently insufficient to heat the semiconductor the point of physical damage or degradation prior to the onset of bulk junction breakdown. As discussed in Part II [27], large superiorities in key SiC electrical and thermal material properties, such as Debye temperature and thermal conductivity [1], are likely to play a key role in making 4H-SiC power devices less susceptible to breakdown damage (bulk or localized) than correspondingly rated silicon power devices.

Upon initial inspection, our results appear to support the assertion in Ref. [19] that certain microplasmas are non-detrimental for 4H-SiC device applications. However, it remains to be ascertained to what degree these results apply to higher voltage SiC pn junctions, as well as other SiC power device topologies. The existence and properties of localized breakdown microplasmas in high-voltage (> 1 kV) SiC devices has not been reported to date. Previous silicon experience suggests that microplasma current is relatively insensitive to junction width and doping [24]. Therefore, it is conceivable that the power density of localized 4H-SiC current filaments may greatly increase as SiC device blocking voltage is increased to 1 kV or 10 kV envisioned for many high-power applications. As will be discussed in Part II [27], there is indirect evidence to suggest that microplasma power density might substantially increase as junction blocking voltage increases. In turn, this could thermally stress higher voltage SiC junctions beyond failure limits that were clearly not reached in these low-voltage 4H-SiC devices.

Prior silicon experience indicates that Schottky rectifiers and bipolar gain devices (such as BJT's, thyristors, IGBT's) are more susceptible to breakdown failure than pn junction rectifiers [16, 17, 28]. It is certainly conceivable that localized breakdown heating at elementary screw

dislocations could damage and fail rectifying metal-SiC Schottky contacts at significantly reduced power levels. The work of Bhatnagar et. al. [29] suggests a plausible link between elementary screw dislocations and reverse leakage non-idealities in SiC Schottky barrier diodes, but as yet there are no published studies explicitly comparing the breakdown properties of well-terminated SiC Schottky barrier diodes with and without elementary screw dislocations. Likewise, the experimental impact of localized SiC breakdown on SiC devices with bipolar gain remains to be investigated.

CONCLUSION

Extensive further studies of elementary screw dislocation defect assisted breakdown are clearly necessary before general quantitative conclusions regarding the reliability of 4H-SiC power devices with elementary screw dislocations can be reached. It is very important that the operational effects of elementary screw dislocations be definitively ascertained, as these defects will be present in all appreciable current (> 1 A) 4H-SiC power devices manufactured on commercial c-axis wafers for the foreseeable future. Therefore, breakdown and switching reliability studies should immediately be undertaken using a variety of existing prototype 4H-SiC devices, both with and without elementary screw dislocations. The resulting data could then be compared with high reliability silicon devices, enabling meaningful extrapolation of the operational reliability of future 4H-SiC power devices with and without elementary screw dislocations relative to present-day silicon high-power devices. An initial such study comparing the dynamic breakdown reliability of low-voltage 4H-SiC rectifiers (with and without screw dislocations) to the dynamic breakdown reliability of silicon pn rectifiers is presented in Part II [27].

ACKNOWLEDGMENTS

The authors would like to gratefully acknowledge the assistance of C. Fazi of U.S. Army Research Laboratory, and D.J. Larkin, J. A. Powell, C. Salupo, G. Beheim, L. Keys, A. Trunek, J. Heisler of NASA Lewis Research Center. Work at NASA Lewis was carried out under joint

funding from NASA Lewis Research Center and Defense Advanced Research Projects Agency (DARPA) Order #D149 (monitored by Dr. J. Alexander) and Order #E111/3 (monitored by Dr. E. Brown). X-ray topography research supported in part by the U.S. Army Research Office under contract numbers DAAH04-94-G-0091 and DAAH04-94-G-0121 (contract monitor, Dr. J. Prater). Topography was carried out at the Stony Brook Synchrotron Topography Facility, beamline X-19C, at the National Synchrotron Light Source, at Brookhaven National Laboratory, which is supported by the U.S. Department of Energy, under contract No. DE-AC02-76CH00016.

REFERENCES

[1] P. G. Neudeck, "Progress in Silicon Carbide Semiconductor Electronics Technology," *J. Electron. Mater.*, vol. 24, no. 4, pp. 283-288, 1995.

[2] M. Bhatnagar and B. J. Baliga, "Comparison of 6H-SiC, 3C-SiC, and Si for Power Devices," *IEEE Trans. Electron Devices*, vol. 40, no. 3, pp. 645-655, 1993.

[3] B. J. Baliga, "Power ICs In The Saddle," *IEEE Spectrum*, vol. 32, no. 7, pp. 34-49, 1995.

[4] G. W. Eldridge, D. L. Barrett, A. A. Burk, H. M. Hobgood, R. R. Siergiej, C. D. Brandt, M. A. Tischler, G. L. Bilbro, R. J. Trew, W. H. Clark, and R. W. Gedridge, Jr., "High Power Silicon Carbide IMPATT Diode Development," American Institute of Aeronautics and Astronautics, Washington, DC June 1993.

[5] P. G. Neudeck and J. A. Powell, "Performance Limiting Micropipe Defects in Silicon Carbide Wafers," *IEEE Electron Device Lett.*, vol. 15, no. 2, pp. 63-65, 1994.

[6] M. Dudley, S. Wang, W. Huang, C. H. Carter, Jr., and C. Fazi, "White Beam Synchrotron Topographic Studies of Defects in 6H-SiC Single Crystals," *J. Phys. D*, vol. 28, pp. A63-A68, 1995.

[7] S. Wang, M. Dudley, C. H. Carter, Jr., V. F. Tsvetkov, and C. Fazi, "Synchrotron White Beam Topography Studies of Screw Dislocations in 6H-SiC Single Crystals", in *Mat. Res. Soc. Proc., vol. 375, Applications of Synchrotron Radiation Techniques to Materials Science,* L. Terminello, N. Shinn, G. Ice, K. D'Amico, and D. Perry, Eds. Pittsburgh, PA: Materials Research Society, 1995, pp. 281-286.

[8] W. Si, M. Dudley, R. Glass, V. Tsvetkov, and C. H. Carter, Jr., "Hollow-Core Screw Dislocations in 6H-SiC Single Crystals: A Test of Frank's Theory," *J. Electron. Mater.*, vol. 26, no. 3, pp. 128-133, 1997.

[9] W. Si and M. Dudley, "Study of Hollow-Core Screw Dislocations in 6H-SiC and 4H-SiC Single Crystals", in *Materials Science Forum, vol. 264-268, Silicon Carbide, III-Nitrides,*

and Related Materials, G. Pensl, H. Morkoc, B. Monemar, and E. Janzen, Eds. Switzerland: Trans Tech Publications, 1998, pp. 429-432.

[10] S. Wang, M. Dudley, C. H. Carter, Jr., and H. S. Kong, "X-Ray Topographic Studies of Defects in PVT 6H-SiC Substrates and Epitaxial 6H-SiC Thin Films", in *Materials Research Society Symposium Proceedings, vol. 339, Diamond, SiC and Nitride Wide Bandgap Semiconductors*, C. H. Carter, Jr., G. Gildenblat, S. Nakamura, and R. J. Nemanich, Eds. Pittsburgh, PA: Materials Research Society, 1994, pp. 735-740.

[11] J. A. Powell, D. J. Larkin, P. G. Neudeck, J. W. Yang, and P. Pirouz, "Investigation of Defects in Epitaxial 3C-SiC, 4H-SiC and 6H-SiC Films Grown on SiC Substrates", in *Institute of Physics Conference Series, no. 137, Silicon Carbide and Related Materials*, M. G. Spencer, R. P. Devaty, J. A. Edmond, M. A. Kahn, R. Kaplan, and M. Rahman, Eds. Bristol: IOP Publishing, 1994, pp. 161-164.

[12] V. F. Tsvetkov, R. C. Glass, D. Henshall, D. A. Asbury, and C. H. Carter, Jr., "SiC Seeded Boule Growth", in *Materials Science Forum, vol. 264-268, Silicon Carbide, III-Nitrides, and Related Materials*, G. Pensl, H. Morkoc, B. Monemar, and E. Janzen, Eds. Switzerland: Trans Tech Publications, 1998, pp. 3-8.

[13] P. G. Neudeck, W. Huang, and M. Dudley, "Breakdown Degradation Associated With Elementary Screw Dislocations in 4H-SiC P+N Junction Rectifiers", in *Materials Research Society Symposia Proceedings, vol. 483, Power Semiconductor Materials and Devices*, S. J. Pearton, R. J. Shul, E. Wolfgang, F. Ren, and S. Tenconi, Eds. Warrandale, PA: Materials Research Society, 1998, pp. 285-294.

[14] S. M. Sze, *Physics of Semiconductor Devices*, 2nd ed. New York: Wiley-Interscience, 1981.

[15] B. J. Baliga, *Modern Power Devices*, 1st ed. New York: John Wiley & Sons, Inc., 1987.

[16] L. W. Ricketts, J. E. Bridges, and J. Miletta, *EMP Radiation and Protective Techniques*. New York: Wiley, 1976.

[17] R. N. Ghose, *EMP Environment and System Hardness Design*. Gainesville, VA: D. White Consultants, 1984.

[18] M. Dudley, "Topography, X-Ray," in *Encyclopedia of Applied Physics*, vol. 21. New York: Wiley-VCH Verlag GmbH, 1997, pp. 533-547.

[19] A. O. Konstantinov, Q. Wahab, N. Nordell, and U. Lindefelt, "Ionization Rates and Critical Fields in 4H SiC Junction Devices", in *Materials Science Forum, vol. 264-268, Silicon Carbide, III-Nitrides, and Related Materials 1997*, G. Pensl, H. Morkoc, B. Monemar, and E. Janzen, Eds. Switzerland: Trans Tech Publications, 1998, pp. 513-516.

[20] K. V. Vassilevski, V. A. Dmitriev, and A. V. Zorenko, "Silicon Carbide Diode Operating at Avalanche Breakdown Current Density of 60 kA/cm^2," *J. Appl. Phys.*, vol. 74, no. 12, pp. 7612-7614, 1993.

[21] K. V. Vassilevski, A. V. Zorenko, and V. V. Novoshilov, "Temperature Dependence of Avalanche Breakdown Voltage of PN-Junctions in 6H-SiC at High Current Density", in *Institute of Physics Conference Series, no. 137, Silicon Carbide and Related Materials: Proceedings of the Fifth International Conference,* Bristol, United Kingdom: IOP Publishing, 1994, pp. 659-661.

[22] P. G. Neudeck, C. Fazi, and J. D. Parsons, "Fast Risetime Reverse Bias Pulse Failures in SiC PN Junction Diodes," presented at Transactions Third International High Temperature Electronics Conference, Albuquerque, NM, 1996.

[23] A. G. Chynoweth and G. L. Pearson, "Effect of Dislocations on Breakdown in Silicon p-n Junctions," *J. Appl. Phys.*, vol. 29, no. 7, pp. 1103-1110, 1958.

[24] A. G. Chynoweth, "Charge Multiplication Phenomena," in *Physics of III-V Compounds*, vol. 4, *Semiconductors and Semimetals*. New York: Academic Press, 1968, pp. 307-325.

[25] A. M. Barnett and A. G. Milnes, "Filamentary Injection in Semi-Insulating Silicon," *J. Appl. Phys.*, vol. 37, no. 11, pp. 4215-4223, 1966.

[26] A. M. Barnett, "Current Filament Formation," in *Injection Phenomena*, vol. 6, *Semiconductors and Semimetals*. New York: Academic Press, 1970, pp. 141-200.

[27] P. G. Neudeck and C. Fazi, "Study of Bulk and Elementary Screw Dislocation Assisted Reverse Breakdown in Low-Voltage (< 250 V) 4H-SiC p^+n Junction Diodes - Part 2: Dynamic Pulse-Breakdown Properties," *IEEE Trans. Electron Devices*, 1999.

[28] D. C. Wunsch and R. R. Bell, "Determination of Threshold Failure Levels of Semiconductor Diodes and Transistors Due To Pulse Voltages," *IEEE Trans. Nucl. Sci.*, vol. 15, no. 6, pp. 244-259, 1968.

[29] M. Bhatnagar, B. J. Baliga, H. R. Kirk, and G. A. Rozgonyi, "Effect of Surface Inhomogenities on the Electrical Characteristics of SiC Schottky Contacts," *IEEE Trans. Electron Devices*, vol. 43, no. 1, pp. 150-156, 1996.

FIGURE CAPTIONS

Figure 1: Cross-section of 4H-SiC p^+n junction diodes tested in this work.

Figure 2: SWBXT back-reflection close-ups of two rectangular 4H-SiC p^+n junction diodes. (a) 240 μm x 100 μm diode containing no elementary screw dislocations. (b) 300 μm x 100 μm diode containing a three elementary screw dislocations. The SWBXT images are slightly compressed by the beam angle along the horizontal direction.

Figure 3: Reverse I-V data comparing 11 diodes with and without elementary screw dislocations.

Figure 4: Low-light optical micrograph of 300 μm x 100 μm diode at 85 V reverse bias showing three breakdown microplasmas that correspond to the three elementary screw dislocations imaged by SWBXT in Figure 2(b).

Figure 5: DC-measured temperature dependence of reverse breakdown I-V of two 50 μm diameter diodes, one without elementary screw dislocations (w/o SD's) and one with two elementary screw dislocations (with SD's). The dashed line represents a theoretical space-charge limited $I \alpha V^2$ fit to the microplasma current (see text).

Figure 6: DC-measured normalized microplasma current I_N versus normalized microplasma voltage V_N. Relation (2) (shown as the thick long-dashed line) reasonably models the DC behavior of breakdown microplasmas observed across the wafer despite significant variations in microplasma turn-on voltage.

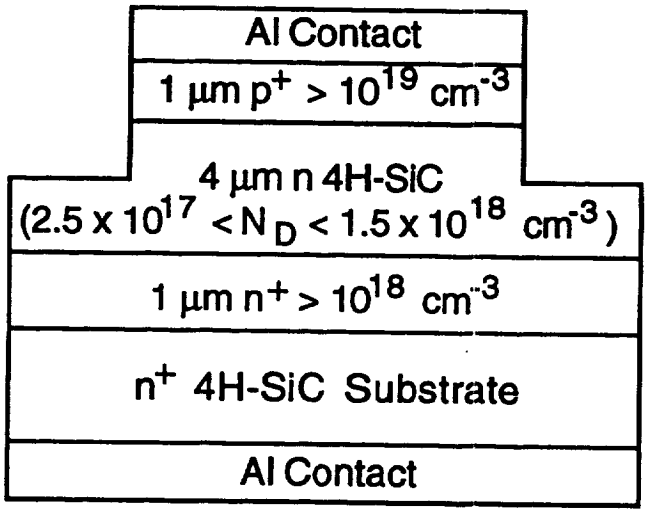
Al Contact
1 μm p+ > 10^19 cm^-3
4 μm n 4H-SiC
(2.5 x 10^17 < N_D < 1.5 x 10^18 cm^-3)
1 μm n+ > 10^18 cm^-3
n+ 4H-SiC Substrate
Al Contact

Figure 1.

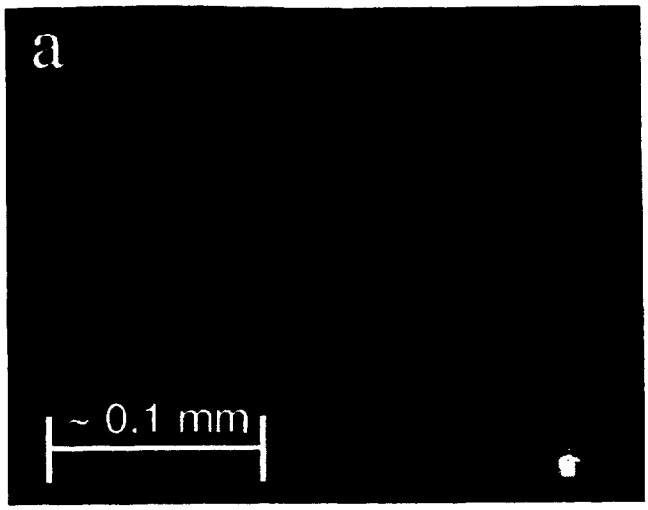

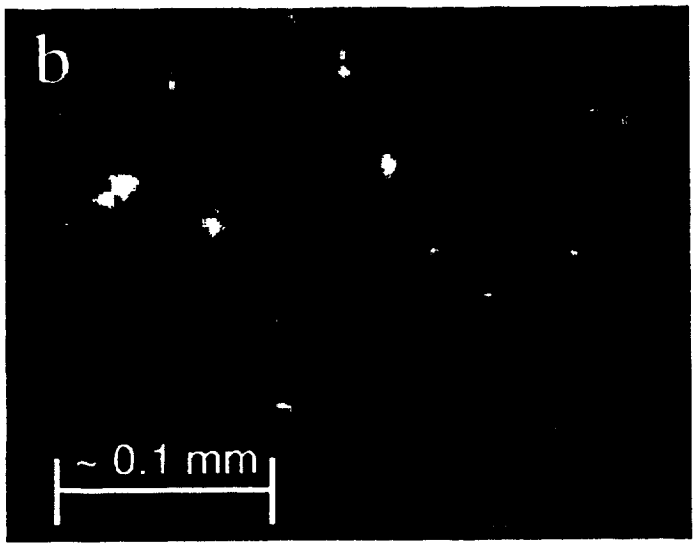

Figure 2

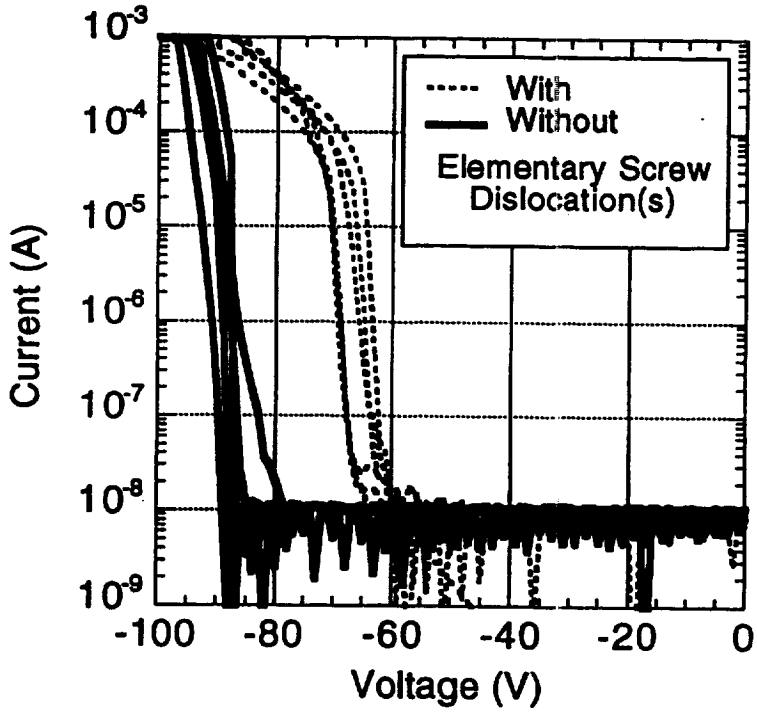
With
Without
Elementary Screw Dislocation(s)
Current (A)
10-3
10-4
10-5
10-6
10-7
10-8
10-9
-100
-80
-60
-40
-20
0
Voltage (V)

Figure 3.

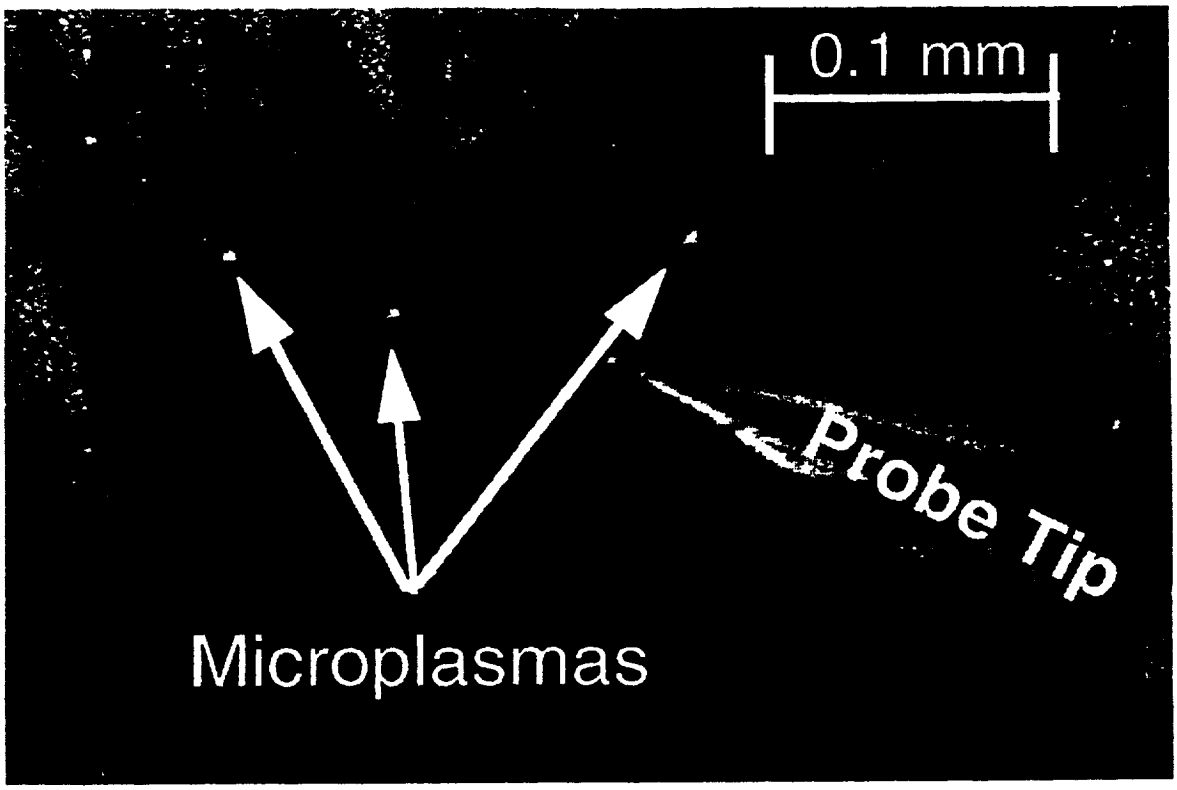

Figure 4

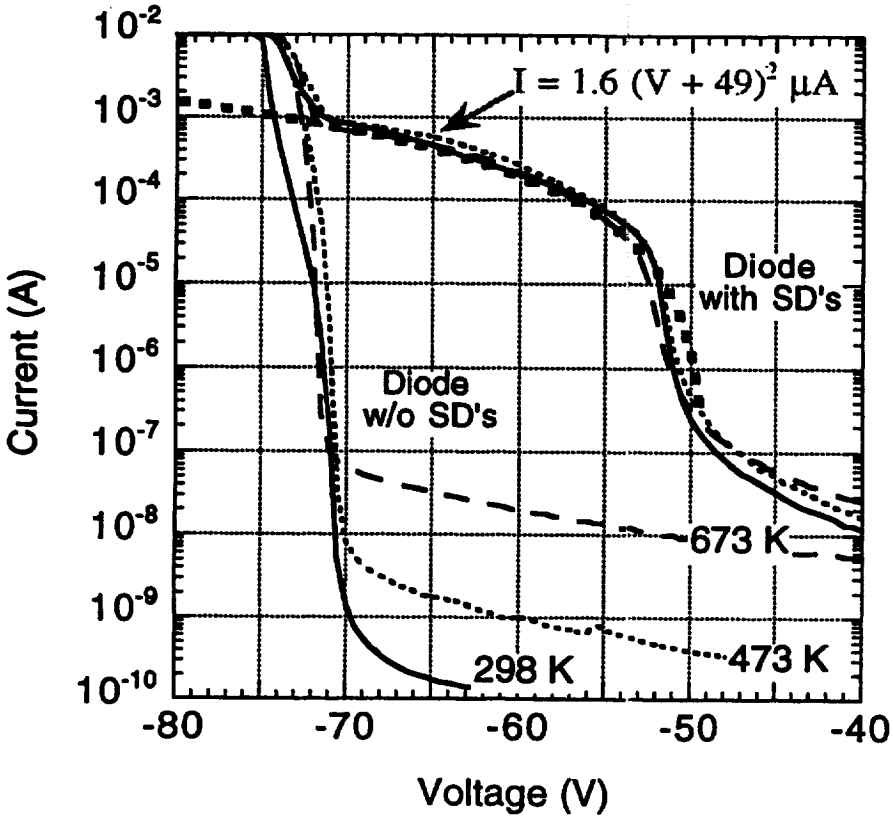
10^{-2}
10^{-3}
10^{-4}
10^{-5}
10^{-6}
10^{-7}
10^{-8}
10^{-9}
10^{-10}
Current (A)
$I = 1.6\ (V + 49)^2\ \mu A$
Diode with SD's
Diode w/o SD's
673 K
473 K
298 K
-80
-70
-60
-50
-40
Voltage (V)

Figure 5

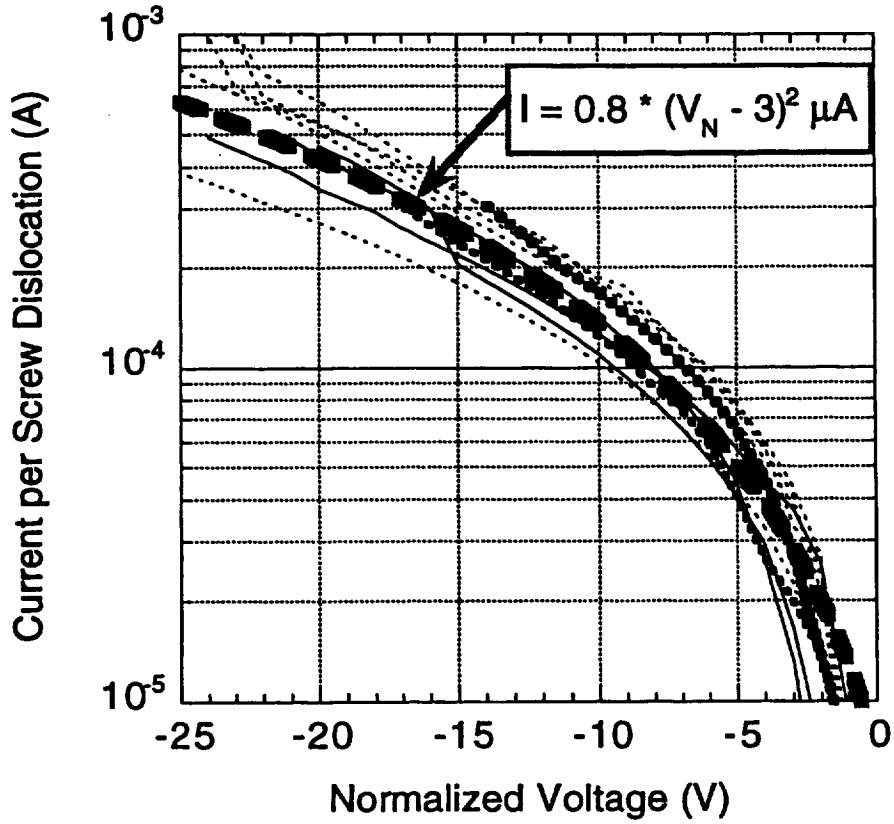
10^{-3}
10^{-4}
10^{-5}
Current per Screw Dislocation (A)
$I = 0.8 * (V_N - 3)^2$ μA
-25
-20
-15
-10
-5
0
Normalized Voltage (V)

Figure 6